PILOT TESTS OF COMPOSITE FLOOR DIAPHRAGMS

M.L. Porter and L.F. Greimann

SYNOPSIS

A facility was designed and fabricated for testing composite floor slabs subjected to large in-plane shear forces. Two full-scale 15 ft (4.58 m) square composite floor slabs were tested. Both specimens were constructed using 3 in. (76 mm) deep corrugated cold-formed steel decking with a 2 1/2 in. (64 mm) superimposed fill of normal weight concrete. The slabs were attached compositely to the support beams of the test facility via stud shear connectors. Specimen 1 was loaded monotonically until reaching the maximum load and followed by incremental displacement further into the nonlinear region. Specimen 2 was loaded cyclically under increasing displacement limits. Both specimens failed as a result of diagonal tension cracking of the concrete. The cyclically-loaded specimen had approximately the same maximum load and stiffness as the monotonically-loaded specimen, but its ductility capacity was less.

RESUME

On a construit un montage expérimental permettant de tester des dalles de planchers composites, soumises à de grands efforts tranchants agissant dans le plan des dalles. Deux dalles de 15 pi. (4.58 m) carrés furent soumises à l'essai. On a construit les deux dalles à l'aide de coffrages en tôles ondulées dont les nervures avaient 3 po. (76 mm) de profondeur, le coffrage étant recouvert de 2½ po. (64 mm) de béton de poids normal. Pour obtenir l'action composite on a attaché les dalles aux poutres du montage avec des goujons. Le premier spécimen fut soumis à des accroissements successifs de la charge jusqu'à la charge maximum, ensuite, dans la zone non linéaire, il fut soumis à des accroissements successifs du déplacement. Le deuxième spécimen fut soumis à un chargement cyclique, augmentant la limite supérieure de la charge durant les cycles de chargement. La rupture des deux spécimens fut causée par la fissuration due à la tension diagonale dans le béton. Le spécimen soumis à un chargement cyclique a atteint la même charge maximum et a démontré la même rigidité que le spécimen soumis à un chargement statique, mais sa ductilité fut moindre.

M. L. Porter and L. F. Greimann are Associate Professors of Civil Engineering, Iowa State University, Ames, Iowa.

INTRODUCTION

General

Composite steel-deck reinforced floor slab systems have developed as a popular floor system over the past decade. These systems have the advantage of reduced labor and material costs and allow for more rapid construction. The steel deck serves as a permanent form during construction and, after the concrete cures on top of the deck, the concrete and deck act together as a composite section in which the steel deck functions as the principal tension reinforcement. A typical system is shown in Fig. 1.

The attachment of the composite slab to the support beams is made using arc spot welds or shear connectors, such as studs or other proprietary devices, welded through the deck to the support beams. If shear connectors are used, composite action is developed between the slab and support beams.

Typically, floor systems are designed to resist gravity (vertical) loads, but they may also be designed to resist in-plane loads. Lateral loads on buildings, such as those due to earthquake and/or wind, cause the floor system to be subjected to in-plane shear forces. The diaphragm acts like a deep beam, spanning between the vertical shear-resisting elements such as shear walls or braced frames.

Objective

An experimental/analytical research program is underway to determine the behavioral characteristics of composite steel-deck floor diaphragms. These characteristics include failure mode, maximum load, ductility and stiffness. The complete research effort includes the design of a diaphragm test facility, full-scale testing of diaphragm composite slab specimens, and development of an analytical model and design equations.

The experimental and analytical work will attempt to define and isolate various failure modes by the selection of the significant parameters that affect the diaphragm behavior. These parameters include deck configuration, support framework, shear connection configuration, concrete variables, specimen configuration and loading program. In this paper the design of the diaphragm test facility and the results of two full-scale composite floor diaphragm tests are discussed. These represent the initial efforts of the complete program. A detailed report of the work summarized here is available [1].

PREVIOUS RESEARCH AND BACKGROUND INFORMATION

A review of previous research on steel deck diaphragms is helpful in understanding the past development and various parameters of diaphragm systems. The first testing of steel deck diaphragms in America was performed in California in 1947 by Johnson and Converse as cited in [2]. The tests utilized corrugated panels and were performed by pulling with cables on a full-sized building. Data from tests conducted in 1949 and 1950 by S. B. Barnes and Associates of California were used in developing design equations found in the Tri-Service design manual entitled Seismic Design for Buildings [3]. In July 1955, the first Cornell University tests of full-scale diaphragm installations were initiated. This work led to the publication of a design guide by the American Iron and Steel Institute (AISI) in 1967 [4]. In 1968, the Steel Deck Institute (SDI) initiated a research program at West Virginia University that resulted in Tentative Recommendations for the Design of Steel Deck Diaphragms [5].

Two types of concrete-filled deck diaphragms are identifiable: noncomposite, in which the steel deck is smooth, and composite, in which the steel deck has some type of mechanical interlock system. Luttrell conducted tests on noncomposite steel deck with low-strength, light-weight concrete fill [6]. Separate tests by S. B. Barnes and Associates investigated both noncomposite and composite diaphragms on a proprietary basis. C. W. Pinkham of S. B. Barnes and Associates developed a set of general design equations for concrete-filled steel deck diaphragms [3]. These equations were initially developed for steel deck diaphragms and later modified for steel deck diaphragms with concrete fill by empirical methods. The equations are based on a limited number of tests and composite requirements are not specified. Several items are unaccounted for in these equations for the design of composite steel deck diaphragm slabs, e.g., stud strength, steel deck configuration, shear-bond, and cyclic loading.

Research at Iowa State University between 1967 and 1977 has been conducted for the purpose of evaluating composite floor slabs reinforced with cold-formed steel decking subjected to gravity loads. A significant result of these vertical load tests was the identification and quantification of a failure mode called shear-bond. These investigations have led to the draft of Tentative Recommendations for Design and Construction of Composite Steel Deck Slabs [7] and [8], and a formulation of the predicted shear-bond strength [9].

DIAPHRAGM TEST FACILITY

Selection of the Test Frame Arrangement

Four primary potential test frame configurations were considered: three-bay simple beam, cantilever with a hinge and roller as supports, diagonally loaded, and cantilever with a very stiff (fixed) edge support. The first two frame types have been adopted by the American Society for Testing and Materials, ASTM [10]. The three-bay simple beam test frame was eliminated because of space and material requirements.

The three remaining potential configurations were analyzed by the finite element method (SAP IV [11]) to compare the relative frame stiffness, diaphragm shear stress distribution, boundary conditions and force input. The cantilever frame with a hinge and roller support, which has been used in most previous diaphragm tests, produced locally high stresses in the area of the hinge support. Previous tests confirmed that failures were initiated at the hinged corner and caused premature concrete cracking. The diagonally-loaded frame provides symmetry about both diagonals and centerlines so that the deck panels have no preferred directions. The diagonal test frame was eliminated, however, because it may not simulate the actual combined bending and shear action present in floor diaphragm systems. The cantilever frame with a fixed edge support was selected as the desired pilot test frame. The fixity along the edge of the diaphragm models an attachment of the slab to a very stiff continuous panel. The stress distribution in this frame model had the least variation in magnitude. Stress distributions were obtained for the fixed edge cantilever test configuration using stiff and flexible support beams. Stiff support beams were selected because they produce a more uniform shear stress in the test diaphragm.

Test Frame Design and Description

The cantilever diaphragm test frame arrangement is shown in Fig. 2. The testing facility consists of three large reinforced concrete reaction blocks, two hydraulic cylinder loading devices with supports, and three perimeter framing beams. The frame was designed for a working load of 400 kips (1780 kN) and a maximum displacement of $\pm$ 6 in. (152 mm). The overall dimensions of the frame are adjustable for various sized specimens and can be repositioned for continuous panel tests. The test frame was initially assembled to accommodate a 15-ft (4.58 m) square specimen. Helpful information on testing techniques, test fixture design, and instrumentation were obtained from [12] and [13].

Three large reinforced concrete reaction blocks were used to support one edge of the diaphragm. An embedded steel plate, simulating a rigid beam flange, was used to attach the steel deck to the concrete blocks. Post-tensioned two-inch diameter bolts provided a friction-type connection to transfer force between the concrete blocks and the laboratory test floor. The edge beams for the test frame were designed and fabricated using W24 x 76 steel framing beams. The edge beams were connected to each other and to the reaction blocks with flexible tee-shaped elements instead of pins or hinges.

Two hydraulic double-acting cylinders were used to apply force into the test frame. The front trunnion-mounted hydraulic actuators were supported by a pair of channels mounted between two beam sections. The lower flange of the beam section was connected to the laboratory test floor by a friction-type connection. Fluorogold slide bearings were used at the ends of the main load beam to resist vertical uplift forces at the corner of the diaphragm.

The test frame was calibrated prior to any testing and again following Test 2. The force required to displace the test frame $\pm$ 5 in.

(127 mm) in both calibration tests was always less than 1.6 kips (7.1 kN). The magnitude of this force was considered small in relation to the test frame capacity (less than instrumentation errors). It was neglected when reducing test data.

Specimen Instrumentation and Description

A schematic layout of the servo-hydraulic control system and data acquisition system is shown in Fig. 3. An axial load cell was connected in series with each hydraulic cylinder. Electrical DCDT (direct current linear variable differential transformers) and mechanical dial gages were used to measure in- and out-of-plane displacements. DCDT's located on the reinforced concrete reaction blocks measured any potential deformation or slip of the fixed reactions. The signal output from the DCDT in the northeast corner was used as a displacement control feedback to the MTS servo-controller on all tests.

Strain gage rosettes were placed on the underside of the steel deck and on the top concrete surface to measure actual steel and concrete strains, respectively. Clip gage rosettes were positioned in the four corners of the diaphragm to measure large strains on the concrete surface after cracking. Slip gages were designed to detect and measure slip of the concrete slab relative to the perimeter framing beams. Strain gages were attached to the web of the perimeter W24 x 76 framing beams. These gages were located such that the axial force and major bending moments could be calculated at selected cross-sections to isolate the forces being transferred into the diaphragm.

A 100-channel data acquisition system was used to record transducer signals on paper and paper-punch tape at various load increments throughout the test. An X-Y recorder and digital voltmeters provided a continuous display of the load and displacement of the loaded beam. An MTS closed-loop control system was used to control displacements during the test.

Specimen Description

Two identical nominal 15-ft (4.58 m) square specimens were constructed for the pilot tests. (Actual out-to-out dimensions of the concrete slab were 15' - 4" x 15' - 4" (4.68 m x 4.68 m).) The pilot test specimens were constructed using 20-gage, 3-in. (76 mm), composite steel-deck panels. The steel decking material had a measured thickness of 0.0336 in. (0.86 mm), a yield point of 41.7 ksi (288 MPa) and an ultimate tensile strength of 53.4 ksi (368 MPa). Figure 4 shows a plan view of the slab, detailing the location of studs, deck panels, seam welds and additional reinforcement. Twice the number of studs than required to develop full slab strength were used to force the failure into the composite slab system itself. Future tests will be conducted with fewer studs, without studs (but with arc-spot welds), with different deck configurations, and with different concrete properties. Additional reinforcing steel (#3, Grade 40 Reinforcing Bar) was used in the edge portion of the rigid reaction side only to prevent a premature failure of the concrete along the stud line. (See Fig. 4).

The concrete was purchased at a local ready-mix plant. The average compressive strength f'_c was 5334 psi (38.9 MPa) and 5250 psi (36.2 MPa) on test day for Specimens 1 and 2, respectively. The concrete slab was shored at midspan for seven days, at which time the shoring beam was removed. Concrete thickness was measured around the perimeter of the slab and at nine locations in the interior of the slab by drilling holes through the concrete. The average thickness of Specimens 1 and 2 was 5 3/8 in. (137 mm) and 5 1/2 in. (140 mm), respectively.

TEST PROCEDURE AND RESULTS

Loading Program and General Behavioral Observations

Specimen 1--The test program was planned so that, after three initial loading reversals at ± 40 kips (178 kN), the specimen was monotonically loaded to the maximum (ultimate) load (in the positive or east direction). The 40-kip (178 kN) load was selected to be approximately equal to the cracking load and was approximately equal to one-fourth the maximum load. Following maximum load, the specimen was displaced further into the nonlinear region.

After achieving a maximum displacement, an investigation was made to determine the behavior of the damaged specimen. Thus, the specimen was unloaded and again subjected to a series of load reversals at approximately one-fourth of the ultimate load. The specimen was next loaded monotonically in the opposite (negative or west) direction until a maximum load was reached. After further displacement in the negative direction, the slab was unloaded and cycled as before. The loading program for Specimen 1 is summarized in Fig. 5 and the corresponding entire load-displacement diagram is shown in Fig. 6.

Figure 7 shows the crack pattern development throughout the test. Small cracks first appeared simultaneously in all four corners of the slab at the end of two and one-half cycles of loading at the 40-kip (178 kN) level, i.e., at Load Point (LP) 12 in Fig. 5. These cracks occurred in the thin portion of the slab at the ends of the deck panels and did not propagate further during the test. At a load of 120 kips (534 kN), diagonal cracks formed in the northeast and southwest corners of the slab at LP #21 as indicated in Fig. 7a. At LP #24 a large diagonal crack occurred in the southwest corner of the slab parallel to the initial diagonal cracks. At this point the servo-valve malfunctioned, the specimen was unloaded to zero load and a backup control system was instituted to complete the test. Loading again resumed at LP #25 starting with an initial reading at zero. A small offset in the initial displacement was experienced after reloading, but the specimen maintained the initial stiffness (See Fig. 6). The maximum load of 168 kips (748 kN) was achieved immediately before LP 30 (shown by the dashed line in Fig. 6). At that point a large diagonal crack developed across the center of the slab (Fig. 7a). The primary failure mode was failure of the concrete in shear due to diagonal tension stresses.

Local deformation of the steel deck corrugations below the concrete cells was observed as the specimen was displaced beyond the

maximum load into the nonlinear region. The downward bending of the deck began in the northwest and southeast corners and progressed inward along the north and south ends of the specimen as displacement was further incremented. Typical deformed corrugations are shown in Fig. 8.

A crack, parallel to the deck corrugations in the thin portion of the concrete above the first flute from the edge, began to develop at LP 34 (Fig. 7b). As the specimen was further displaced the crack continued to propagate and a similar parallel crack developed in the northwest corner (LP 36). The top flanges of the edge beams and the narrow edge section of cracked concrete rotated outward. Figure 7c shows the crack pattern as observed at maximum positive displacement (LP 30). After the specimen was unloaded and cycled, it was loaded in the reverse (negative or west) direction until the maximum load of -122 kips (543 kN) occurred just after LP 53. A large diagonal crack occurred across the control region of the slab from the northeast to the southwest corners. At this load, the top flanges of the framing beams in the northeast and southwest corners of the test frame rotated outward, similar to the action which occurred under positive loading at LP 40. Fig. 7d shows the crack pattern at the end of the test.

Specimen 2--Specimen 2 was subjected to cyclic loading with progressively increasing displacement limits. The initial displacement limit was $\pm$ 0.05 in. (1.3 mm), followed by limits of $\pm$ 0.10, $\pm$0.20, $\pm$0.30, $\pm$0.50, $\pm$0.75 and $\pm$1.00 in.(0.5, 5.1, 7.6, 12.7, 19.1 and 25.4 mm), respectively. Three displacement cycles were applied within each limit. Figure 9 shows the entire load-displacement diagram.

Generally, the crack pattern for Specimen 2 (Fig. 10) was similar to that of Specimen 1, except diagonal cracks developed in all four corners of the slab. The maximum positive load of 186 kips (828 kN) occurred immediately before LP 38 and the maximum negative load of -165 kips (734 kN) occurred between LP 41 and LP 42. The dashed lines in Fig. 9 represent the maximum loads. The primary failure mode in both directions was diagonal tension cracking resulting from shear forces (Fig. 10). At displacement reversals beyond the maximum load, the steel deck corrugations began to bend out-of-plane similar to the behavior which occurred in Specimen 1. North-south cracks, parallel to the deck corrugations, developed parallel to the east and west edges of the slab similar to Specimen 1. The top flanges of the east and west framing beams had rotated outward in all four corners, similar to the behavior observed in Specimen 1.

Summary of Data

A detailed presentation and interpretation of all the data from these two tests is beyond the scope of this paper; however, general observations are summarized in this section.

In general, concrete shear strains were in proportion to the load history of the specimens but decreased in magnitude after the major central diagonal crack formed. The strain gage rosettes on the steel deck showed that a more significant force was transferred into the steel deck following the major diagonal crack. The strains

in the steel deck resulted from diagonal tension forces and flexural forces due to out-of-plane displacements. No significant straining occurred in the steel deck until after the concrete cracked. This is analogous to the behavior of web reinforcement in a reinforced concrete beam in which the web steel has little or no noticeable effect prior to the formation of diagonal cracks. However, the deck in these tests did not perform as conventional shear reinforcement after major cracking because the slab system carried no increased load.

The slip gages, as well as visual observation, indicated that slip between the steel deck and concrete did not occur. Shear studs confined the concrete before and after cracking, preventing slip.

The vertical (out-of-plane) deflections generally cycled in phase with the load history. Both specimens deflected downward prior to the maximum load and then displaced upward (i.e., less downward total deflection) immediately following the maximum load and the formation of the crack through the main diagonal of the slab. As the specimen was subjected to an increased number of displacement cycles, the out-of-plane deflections increased (in a downward direction).

The strain gages attached to the perimeter steel framing beams were used to determine the axial force and moment at various cross-sections along the beams. If a uniform transfer of shear occurs between the load beams and slab, the axial force distribution along the edge beams will be linear. The experimentally determined axial force distribution illustrated that this general behavior was in the linear range. As the specimens were displaced into the nonlinear region, the axial force distribution in the east and west framing beams became more uniform rather than linear, varying from zero to a maximum.

EVALUATION OF RESULTS

Evaluation of the Test Facility

The test frame performed very well, as evidenced by the symmetry in the crack patterns and instrumentation. No slippage occurred in the reinforced concrete reaction blocks or at the hydraulic cylinder supports, and support deformations were small enough to be considered negligible. The flexible tee connections were satisfactory and are a desirable substitute for pinned connections. When compared to the finite element distribution, the in-plane experimental concrete shear strain distribution showed that the frame and diaphragm behaved about as predicted. Except for minor problems, the instrumentation performed quite well.

Specimen Behavior

Failure modes and loads--the primary mode of failure for both specimens was diagonal tension cracking. No experimentally-verified technique is yet available for predicting this failure for composite slabs. In certain respects, the diaphragm behavior was similar to a deep beam or wall, i.e., the failure mode was a classic diagonal crack. The steel deck (shear reinforcement)underwent no significant straining

until after major cracks occurred.

If the diaphragm can be assumed to be a deep beam without shear reinforcement, Equations (11-29), ACI 318-77 [14] can be used to calculate the shear strength. At least three additional assumptions seem reasonable:

1. The average thickness of the slab can be used since the diagonal crack length is large relative to the corrugation length.

2. The critical section is selected at the support since the usual support compressive forces associated with top loading (ACI 318-77, 11.8.1) do not exist.

3. The W24 x 76 edge beams act as bending reinforcement similar to reinforcing bars in a deep beam since the beams are intimately connected to the concrete via studs. Thus, ρ_w is calculated as the area of the W24 x 76 divided by $b_w d$.

The deep beam strength is tabulated in Table 1. The shear strength of the deck, V_s, has been taken equal to zero.

The diaphragm could also be analyzed as a shear wall without shear reinforcement. If the effective depth, d, is taken equal to the distance from the extreme compression force to the resultant of the tension force, i.e., $d = l_w$ [15], and the normal axial force is taken equal to zero, Equations (11-33) and (11-34) ACI 318-77 [14] can be used to calculate the shear strength tabulated in Table 1.

Both the ACI deep beam and shear-wall equations give good results for the maximum load if the deck is not considered as shear reinforcement. Since the diaphragm loads were introduced and reacted by an in-plane line load, a shear-wall model more correctly satisfies the equation assumptions than does a deep beam model [16]; thus, the shear-wall formulation is preferred for the analysis of the mode of failure encountered in these tests. The efficiency of the steel deck as shear reinforcement is diminished somewhat because the deck does not have the development characteristics of ordinary steel reinforcing bars. However, the steel deck does add to the ductility capacity of the slab system.

Ductility--As illustrated in Figs. 6 and 9, neither specimen exhibited the classic ductile behavior desirable for seismic applications. In other words, the load did not remain constant but decreased with increased displacements beyond the displacement at the maximum load; thus, strain softening existed. However, the results suggest that the system will maintain a significant load at large displacements. Two mechanisms appear to be responsible for this reserve load capacity. First, the steel deck behaves somewhat like shear reinforcement in a conventional reinforced concrete beam in that it can transmit tensile forces across the concrete crack. Second, a compressive strut type action is possible in this system [16]. The edge beams act as the chord members of a truss while the concrete acts as a diagonal compressive

truss member parallel to the crack. The axial force distribution in the edge beams, after the maximum load, was consistent with the truss mechanism (i.e., for a positive displacement, the west and north beams [tensile chord members] developed approximately uniform axial tensile forces, while the east beam axial force approached zero).

Ductility is usually defined as the ratio of the maximum displacement to the displacement at yield, Δ_{max}/Δ_y[17]. In a system, such as that considered here, which does not exhibit the classic elastic-perfectly plastic behavior, a definition of the yield displacement is somewhat arbitrary. Yielding (of the steel) was not detected in the testing of Specimens 1 and 2. For the present purposes, yield load, P_y, and yield displacement, Δ_y, will be defined as equal to the yield point of an equivalent elastic-perfectly plastic system (Fig. 11). Since energy absorption characteristics are an important seismic consideration, the equivalent system will be defined to have the same energy content as the real system up to the maximum displacement, Δ_{max} [18, 19]. With this definition, the yield force and ductility may be calculated for any selected maximum displacement. Figure 12 illustrates the relationship between the yield force and the ductility capacity of the equivalent elastic-perfectly plastic system for Specimens 1 and 2. For Specimen 2 (Fig. 9), an envelope curve, which enclosed the third cycle in each displacement increment, was used to calculate the energy for the equivalent system.

Design considerations--Two design possibilities are suggested at this stage of the research program: (1) consider the system to be brittle (ductility equals 1) and use a large factor of safety, say 3 or 4, on the ultimate load; and/or (2) consider the system to be ductile (ductility of perhaps 10) and use a smaller factor of safety, say 1.7, on the yield load from Fig. 12. These and other possible design criteria will be studied as more research is conducted.

Stiffness--The shear stiffness (load/shear displacement) for both specimens was determined using the procedures outlined in ASTM A455-76 [10] and the AISI publication Design of Light Gage Steel Diaphragms [4]. Calculated shear stiffnesses were 2800 and 3100 kips/in. (490 and 540 kN/mm), respectively.

An average cyclic stiffness was determined by calculating the slope of a line extending between the maximum positive and negative load-displacement values of the third cycle hysteresis loops [20]. Specimen 1 had an initial cyclic stiffness (load/total displacement) of 1810 kips/in. (317 kN/mm). After it was displaced to a maximum of 1.00 in. (25.4 mm) and subjected to a series of load reversals, the stiffness had deteriorated to 230 kips/in. (40 kN/mm). The final cyclic stiffness calculated near the end of the test was 220 kips/in. (39 kN/mm). An important observation in Test 2 was the degradation of stiffness and strength occurring at the peak displacements as the specimen was subjected to load reversals in the nonlinear range (Fig. 9). The stiffness of Specimen 2 degraded from an initial cyclic value of 2000 kips/in. (350 kN/mm) to about 70 kips/in. (12 kN/mm). The most significant deterioration in stiffness occurred following the maximum load.

The deterioration in stiffness within each hysteretic loop, i.e., the change in slope near the point of zero load, was caused by a phenomenon known as shear pinching [21]. Shear pinching behavior is a result of the change in restraint provided by the steel deck and the aggregate interlocking along the concrete cracks. As the specimen is subjected to an increased number of load reversals, the aggregate interlock deteriorates and offers less resistance; thus, the stiffness is reduced.

Loading history--Specimen 1 was tested monotonically, whereas Specimen 2 was tested cyclically to study the influence of the loading reversals on the strength, stiffness, ductility and failure modes. Figure 13 shows an envelope of the load-displacement diagrams for the two specimens. The envelope of Specimen 2 utilizes the results of the third cycle in each displacement increment. A comparison of these two curves shows that the curve obtained under monotonic loading, Specimen 1, provides an upper bound envelope curve for the hysteretic behavior obtained from the cyclic loading. The primary failure mode in both specimens was failure of the concrete by diagonal tension. The maximum loads achieved in both tests were within 10% (Table 1). Specimen 2 had a lower ductility capacity than did the monotonically loaded Specimen 1, Fig. 12. The initial stiffness for both specimens was approximately the same. The cyclic loading program was more severe for testing specimens in shear because the stiffness and strength of the specimen deteriorated after each loading reversal in the nonlinear range (Fig. 9). A cyclic loading program will be used for future tests.

SUMMARY AND CONCLUSIONS

A facility was designed and constructed for testing composite floor slabs acting as diaphragms. The facility included a cantilever-type test frame with two hydraulic cylinders that applied an in-plane shear load to the specimen. One edge of the specimen was attached to large concrete reaction blocks, thus simulating a fixed support. Instrumentation associated with the test facility included load cells, displacement transducers, strain gages, clip gages and slip gages. The test facility performed quite well.

Two pilot test floor slab specimens were constructed identically with normal weight concrete superimposed on a 3-in. (76 mm) deep composite-type steel deck. Stud shear connectors were used to attach the floor system to the support beams. Specimen 1 was loaded monotonically and Specimen 2 was loaded cyclically to observe the effect of the loading program on the specimen behavior. The failure mode for both specimens was diagonal tension cracking of the concrete. The maximum strength of the diaphragm was calculated using the ACI deep-beam and shear-wall equations [14], which gave good results for predicting the maximum load while neglecting the steel deck as shear reinforcement. Because of closer coordination with the equation assumptions, the shear-wall formulation was concluded to be a better predictor for the failure mode encountered. The cyclic load program of Specimen 2 did not affect the maximum load capacity of the floor slab system.

The diaphragm was able to sustain a significant load after reaching the maximum and after displacement into the nonlinear region. The steel deck did not appear to contribute significantly to the strength of the system but it probably increased the ductility capacity. The cyclically-loaded Specimen 2 had a lower ductility capacity than the monotonically-loaded Specimen 1.

The stiffness for both specimens was approximately the same in the linear region, but deteriorated near the end of testing to less than 10%.

The monotonic loading provided an upper bound envelope load-displacement curve for the hysteretic behavior obtained from the cyclic loading. A shear pinching phenomenon was observed in the cyclic hysteresis curves. In general, the cyclic loading program was considered more severe for testing specimens subjected to shear.

RECOMMENDATIONS

The cyclic load program is preferred for testing diaphragm shear specimens. For future tests, the specimens should be subjected to enough displacement cycles to produce sufficiently stable hysteresis loops. Since the failure of Specimens 1 and 2 was forced into the slab itself by the use of a large number of shear studs, future tests with fewer studs (including no studs), as well as various other parameters, will be performed to evaluate other potential failure modes.

ACKNOWLEDGMENTS

This research on the earthquake resistance of composite steel-deck-reinforced diaphragms was conducted by the Engineering Research Institute at Iowa State University through funds made available by the National Science Foundation Grant No. ENV75-23625. The authors wish to thank the steel deck supplier, the Nelson Stud Welding Company, and Fluorocarbon Company for their contributions to the project. Graduate students G. L. Krupicka, D. J. Brangwin, and especially V.E. Arnold contributed greatly to this particular work.

REFERENCES

1. Arnold, V. E., Greimann, L. F., and Porter, M. L., Pilot Tests of Composite Floor Diaphragms, Progress Report to National Science Foundation, Grant No. ENV75-23625, September 1978.

2. Nilson, A. H., "Shear Diaphragms of Light Gage Steel," Journal of the Structural Division, ASCE, Vol. 86, No. ST11, November 1960, pp. 111-140.

3. Department of the Army, Navy, and the Air Force, Seismic Design of Buildings, Army TM5-809-10, U.S. Government Printing Office, Washington, D.C., April 1973.

4. American Iron and Steel Institute, Design of Light Gage Steel Diaphragms, AISI Committee on Building Research and Technology, Washington, D.C., 1967.

5. Steel Deck Institute, Tentative Recommendations for the Design of Steel Deck Diaphragms, The Steel Deck Institute, Westchester, Illinois, October 1972.

6. Luttrell, L. D., "Shear Diaphragms with Lightweight Concrete Fill," Proceedings of First Specialty Conference on Cold-Formed Steel Structures, Department of Civil Engineering, University of Missouri-Rolla, August 19-20, 1971.

7. American Iron and Steel Institute, Draft of Tentative Recommendations for Design and Construction of Composite Steel Deck Slabs, Unpublished report, Washington, D.C., 1977.

8. Porter, M. L. and Ekberg, C. E., Jr., "Design Recommendations for Steel Deck Floor Slabs," Journal of the Structural Division Proceedings of the American Society of Civil Engineering, Vol. 102, No. ST11, Proceedings paper 12528, November 1976, pp. 2121-2136.

9. Porter, M. L., Ekberg, C. E., Jr., Greimann, L. F., and Elleby, H. A., "Shear-Bond Analysis of Steel-Deck-Reinforced Slabs," Journal of the Structural Division Proceedings of the American Society of Civil Engineering, Vol. 102, No. ST12, Proceedings paper 12611, December 1976, pp. 2255-2268.

10. ANSI/ASTM E455-76, "Standard Test for Static Load Testing of Framed Floor or Roof Diaphragm Construction for Buildings," American Society for Testing and Materials, Vol. 18, 1976, pp. 826-831.

11. Bathe, K. J., Wilson, E. L., and Peterson, F. E., SAP IV Structure Analysis Program for Static and Dynamic Response of Linear Systems, Report No. EERC 73-11, University of California at Berkeley, April 1974.

12. Bertero, V. V., Popov, E. P., Endo, T., and Wang, T. Y., "Pseudo-Dynamic Response of Structures," ASCT/EMD Specialty Conference, University of California at Los Angeles, March 1976.

13. Wang, T. Y., Bertero, V. V., and Popov, E. P., Hysteretic Behavior of Reinforced Concrete Framed Walls, Report No. EERC 75-23, University of California at Berkeley, December 1975.

14. American Concrete Institute, Building Code Requirements for Reinforced Concrete, (ACI Standard 318-77), American Concrete Institute, Detroit, 1977.

15. Cardenas, A. E., Hanson, J. M., Corley, W. G., and Hognestad, E., "Design Provisions for Shear Walls," Journal of the American Concrete Institute, Proceedings 70, No. 3, March 1973, pp. 221-230.

16. Park, R. and Paulay, T., Reinforced Concrete Structures, John Wiley and Sons, Inc., New York, 1975.

17. Mahin, S. A. and Bertero, V. V., "Problems in Establishing and Predicting Ductility in a Seismic Design," International Symposium on Earthquake Structural Engineering, University of Missouri-Rolla, August 19-21, 1976.

18. Biggs, J. M., Introduction to Structural Dynamics, McGraw-Hill Book Co., New York, 1964.

19. Burdette, E. G. and Bernal, D., "Ductility Ratio for Slabs," Journal of the Structural Division, ASCE, Vol. 104, No. ST11, November 1978, pp. 1741-1748.

20. Clough, R. W. and Oenzien, J., Dynamics of Structures, McGraw-Hill Book Co., New York, 1975.

21. Celebi, Mehmet, "On the Shear Pinched Hysteresis Loops," International Symposium on Earthquake Structural Engineering, University of Missouri-Rolla, Vol. 1, August 19-21, 1976.

NOTATION

b_w = Web thickness of diaphragm used for deep beam calculations (applied as distance from the top of the slab to the deck c.g.s. for ACI calculations, i.e., = h)

d = Distance from extreme compression fiber to centroid of tension reinforcement

f'_c = Compressive strength of concrete

h = Thickness of the diaphragm utilized for shear wall calculations

l_w = Horizontal length of wall for shear wall calculations

P = Total shear force applied to the diaphragm

P_u = Maximum total shear force applied to the diaphragm

P_y = Shear force applied to diaphragm at the yield displacement

V_s = Shear strength provided by shear reinforcement

V_u = Maximum shear force at failure section

Δ = Total diaphragm deflection

Δ_{max} = Maximum diaphragm displacement at a specified yield load

Δ_y = Diaphragm displacement corresponding to the yield load

ρ_w = $A_s/b_w d$, where A_s is the area of tension reinforcing steel

Table 1. Summary of specimen strength.

	Specimen 1	Specimen 2
Analytical (ACI 318-77)		
f'_c	5634 psi (38.9 MPa)	5250 psi (36.2 MPa)
b_w, h	3 7/8 in. (98 mm)	4 in. (102 mm)
d	180 in. (4.58 m)	180 in. (4.58 m)
V_u, deep beam (ACI 318-77, Eqs. 11-29)	155 kips (690 kN)	155 kips (690 kN)
V_u, shear wall (ACI 318-77, Eqs. 11-33)	173 kips (770 kN)	172 kips (765 kN)
Experimental		
V_u	168 kips (748 kN)	186 kips (828 kN)

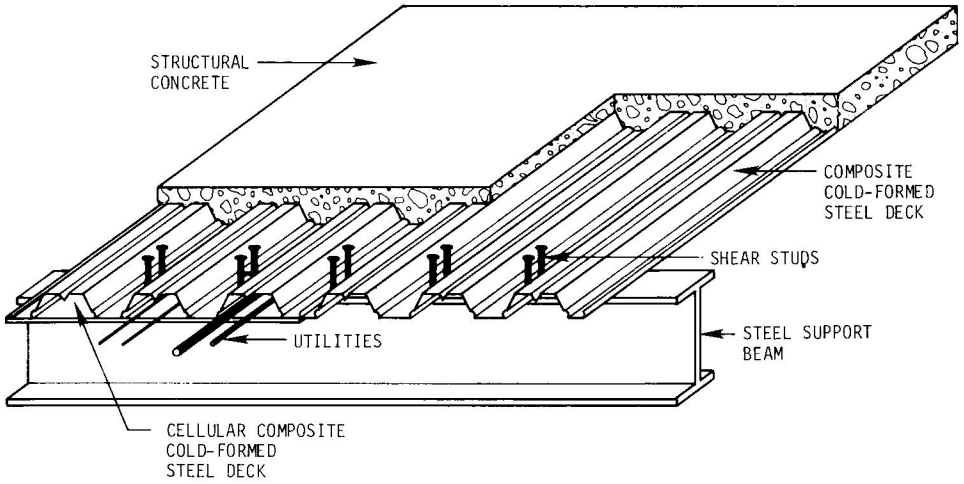

Fig. 1. Typical construction utilizing cold-formed steel decking with composite support beams.

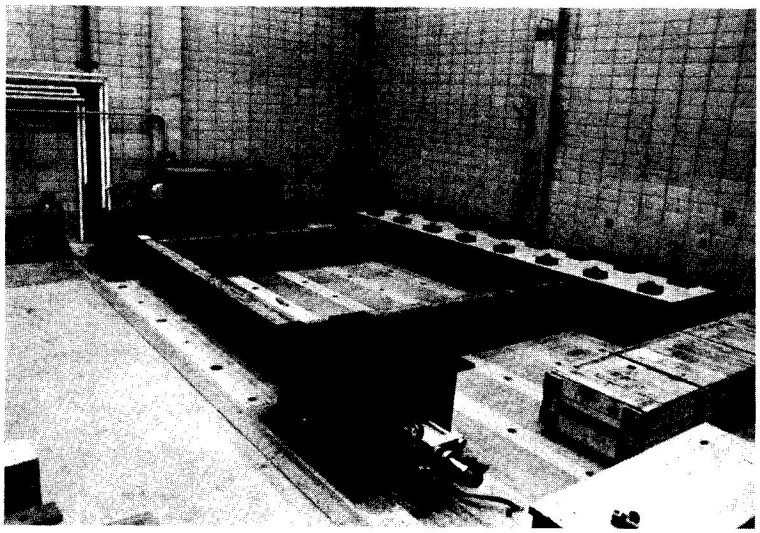

Fig. 2. Overview of diaphragm test facility.

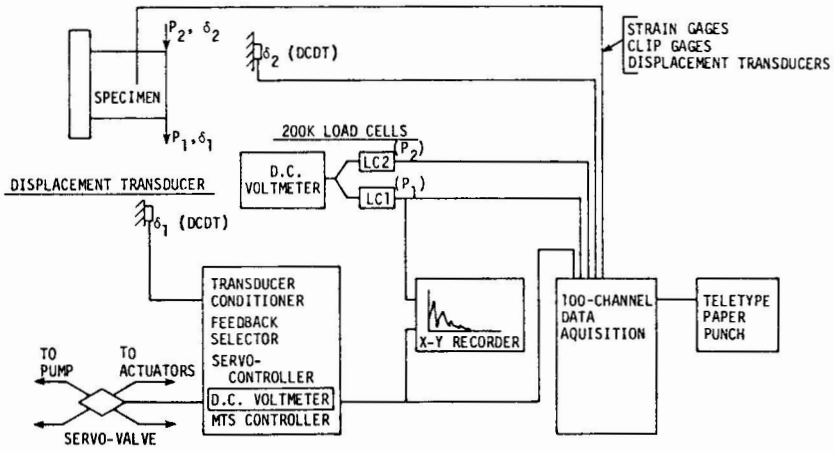

Fig. 3. Servo-hydraulic testing system.

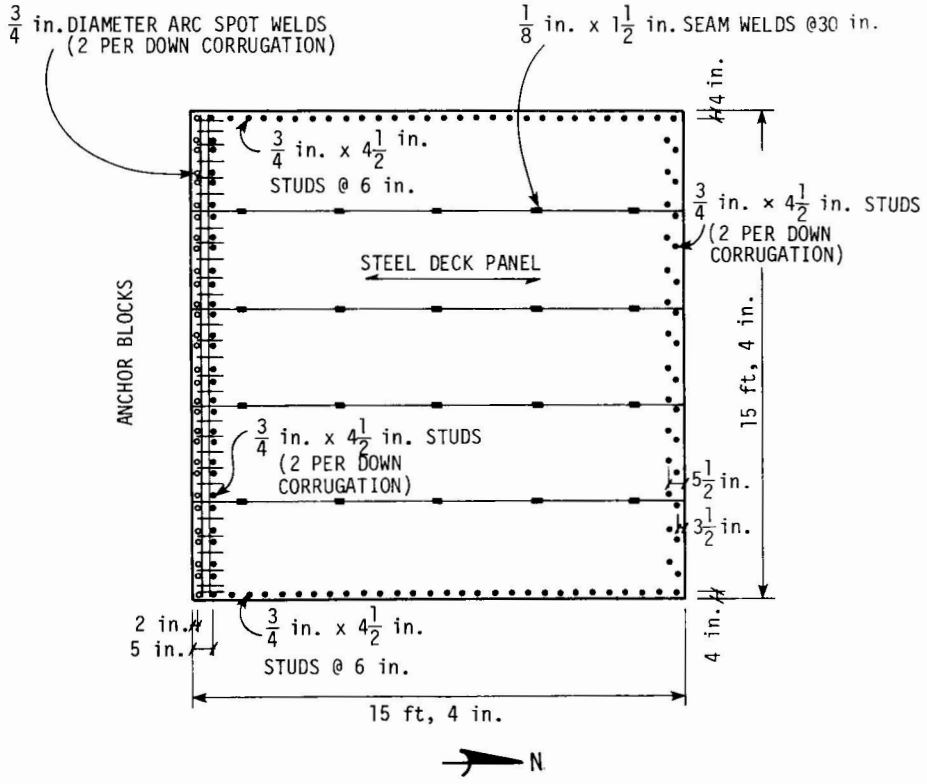

Fig. 4. Detailed plan view of pilot test Specimens 1 and 2 (1 ft = 0.304 m; 1 in. = 0.0254 m).

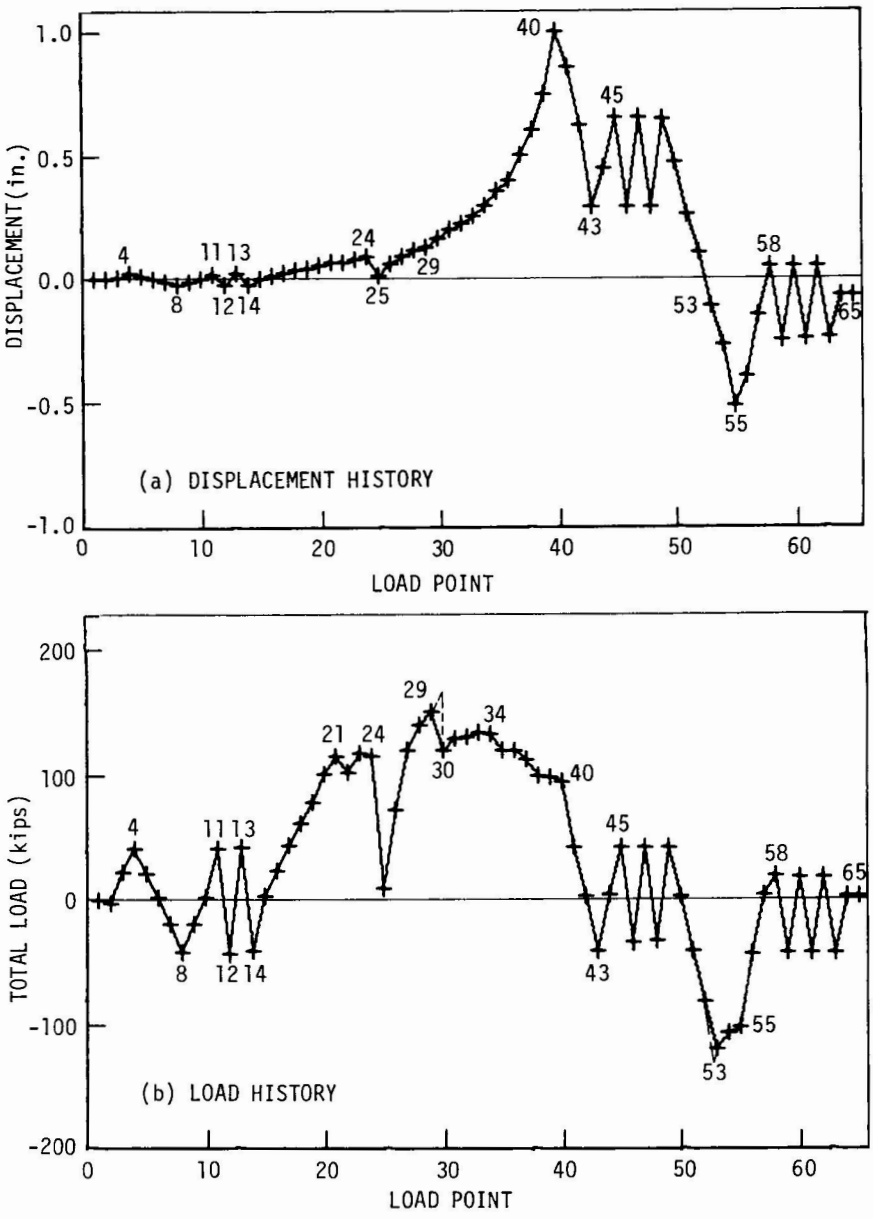

Fig. 5. Loading program--Specimen 1 (1 kip = 4.45 kN; 1 in. = 25.4 mm).

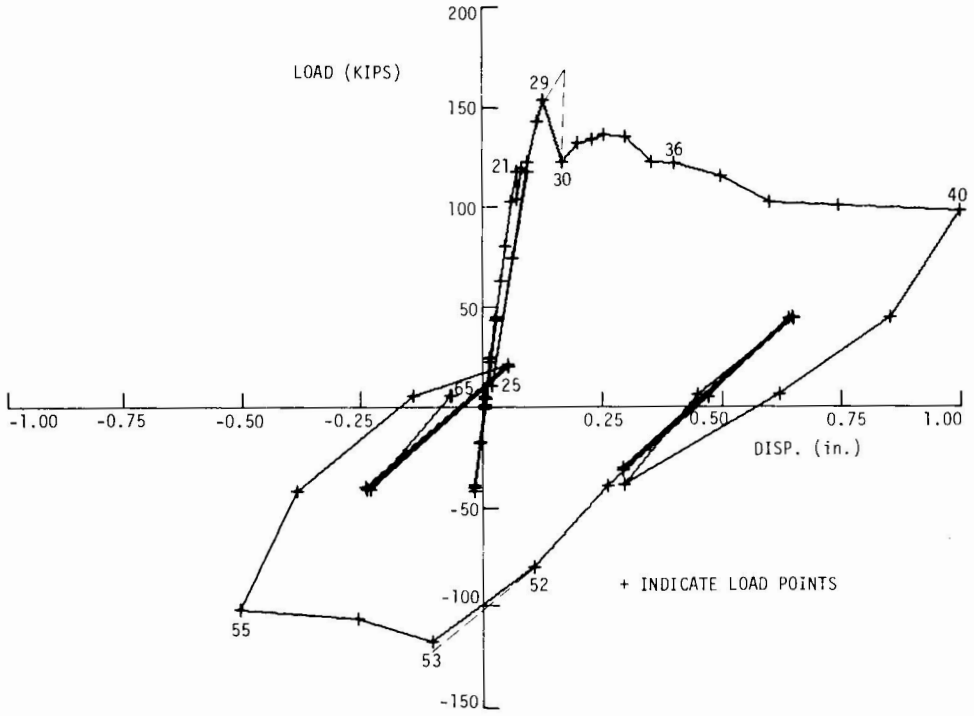

Fig. 6. Load-displacement diagram--Specimen 1 (1 kip = 4.45 kN; 1 in. = 25.4 mm).

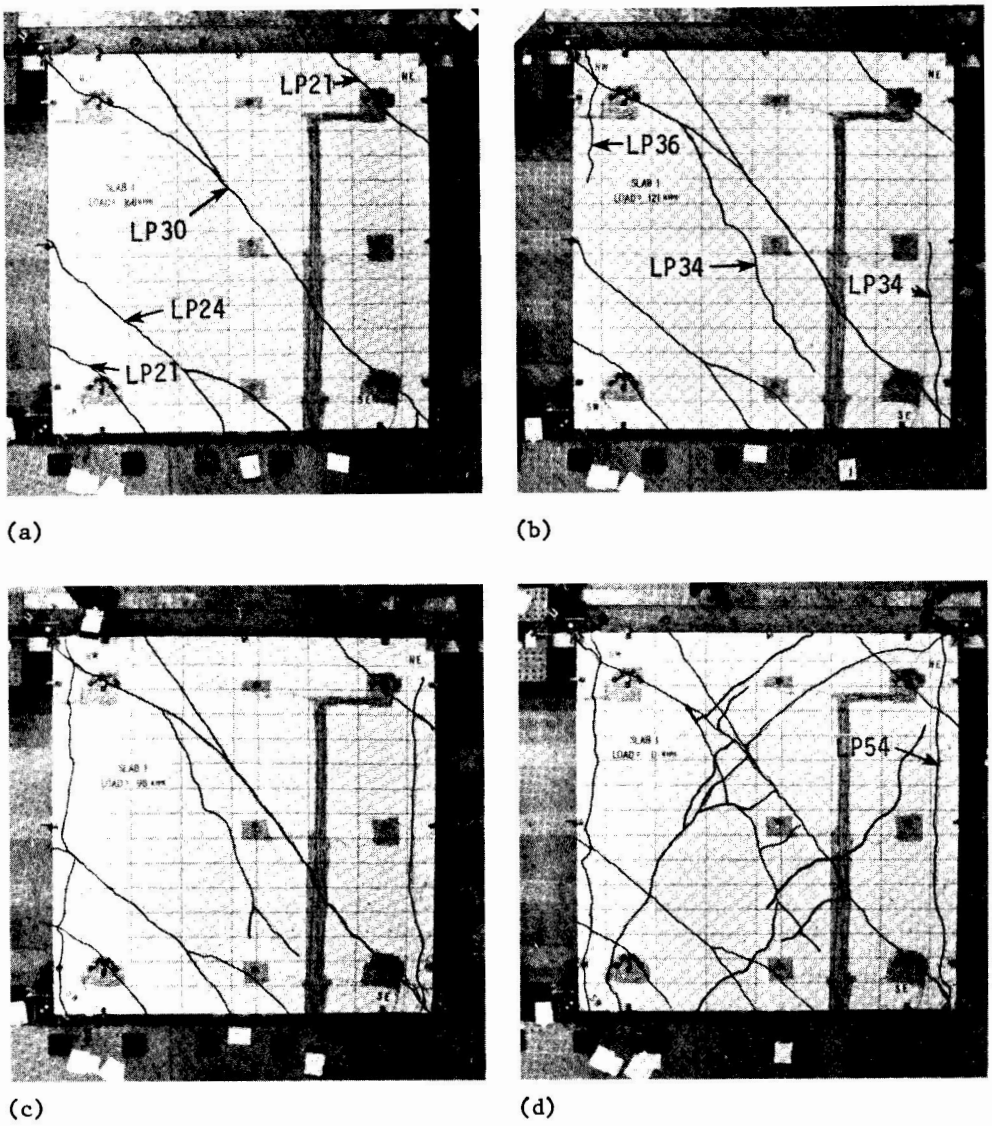

Fig. 7. Crack history for Specimen 1 (north is up; positive displacement is east).
(a) Maximum load (LP 30)
(b) Cracks parallel to deck corrugations (LP 36)
(c) Maximum positive displacement (LP 40)
(d) End of test (LP 65)

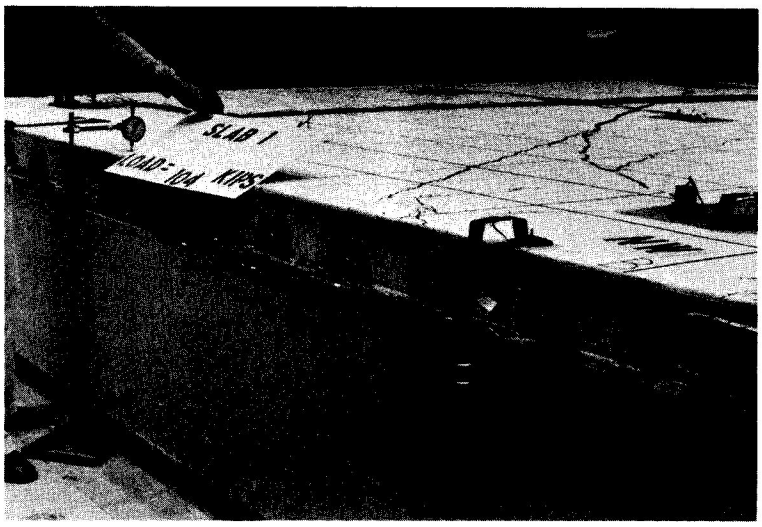

Fig. 8. Local deformation of the steel deck corrugations (LP 38) (view of north edge).

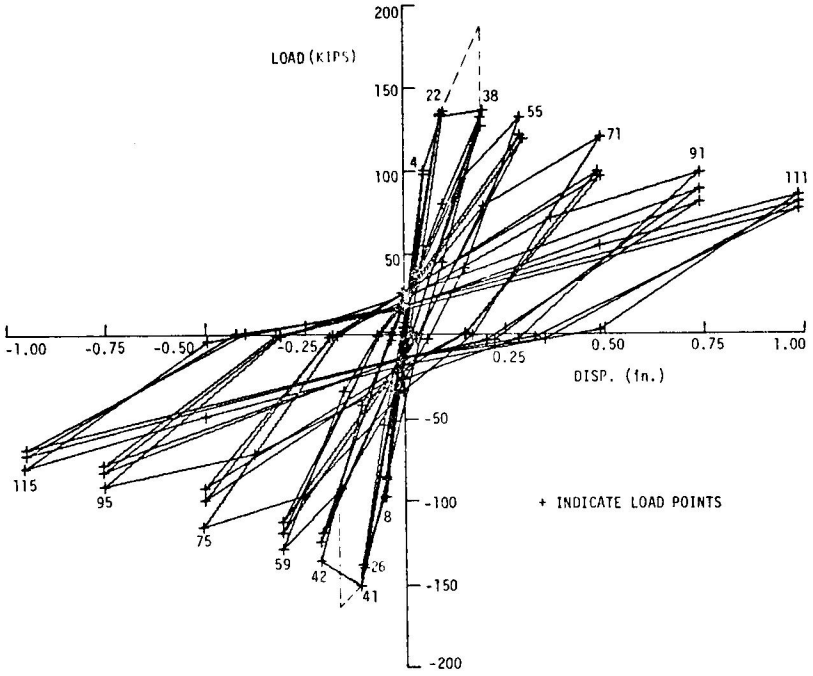

Fig. 9. Load-displacement diagram--Specimen 2 (1 kip = 4.45 kN; 1 in. = 25.4 mm).

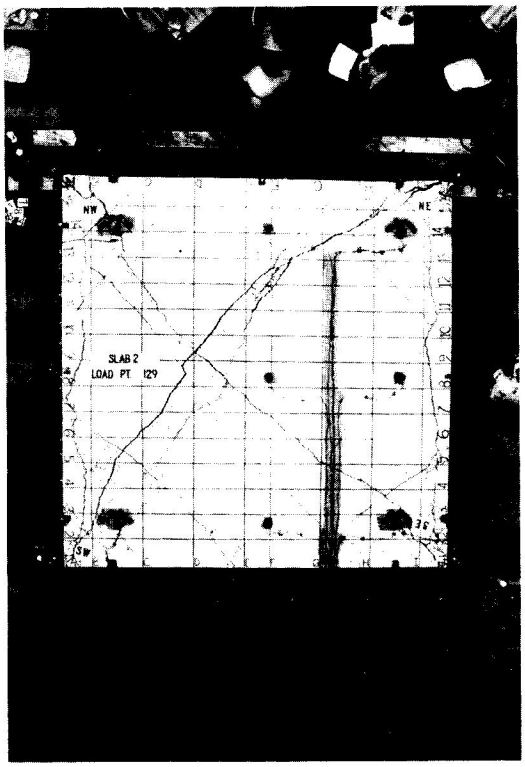

Fig. 10. Final crack pattern for Specimen 2 (north is up; positive displacement is east).

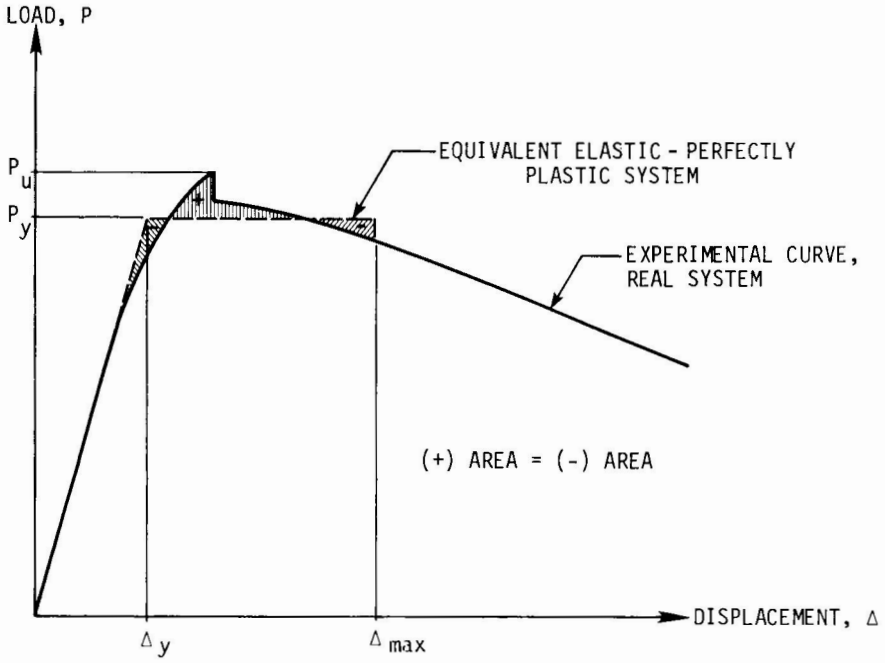

Fig. 11. Equivalent elastic-perfectly plastic system.

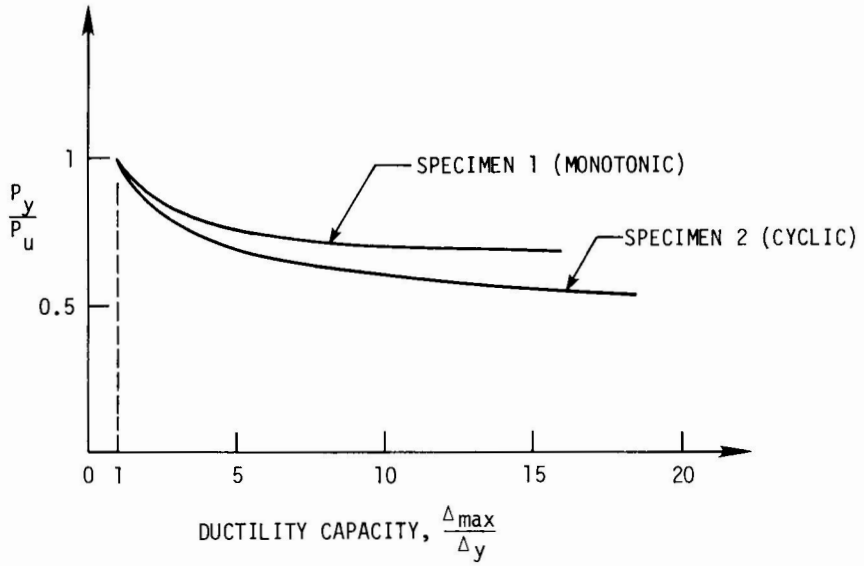

Fig. 12. Ductility capacity.

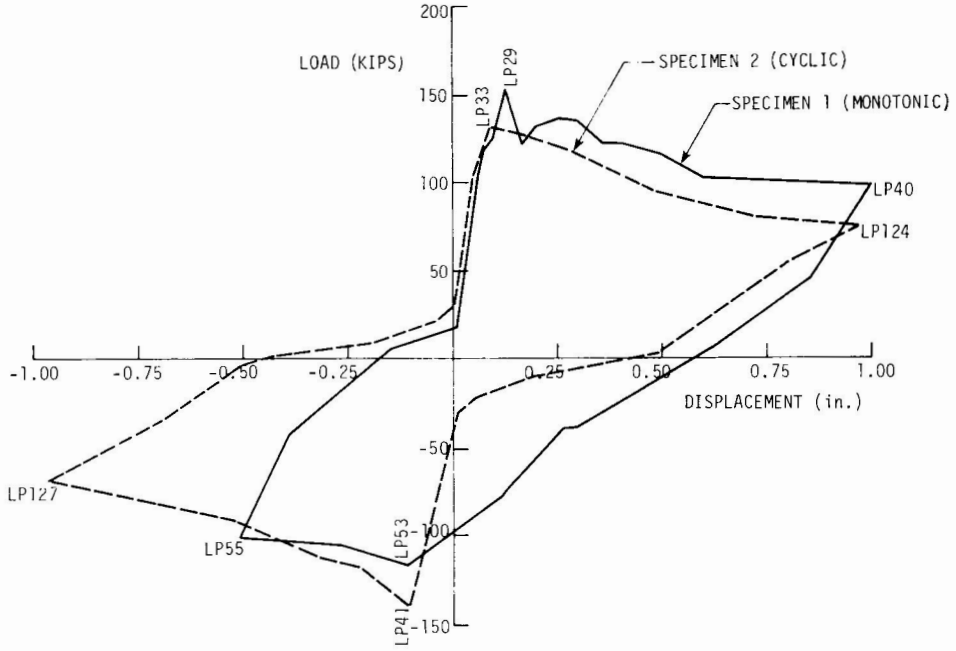

Fig. 13. Envelope curve of load-displacement for Specimens 1 and 2 (1 kip = 4.45 kN; 1 in. = 25.4 mm).